Journal of Sound and Vibration (2000) **230**(1), 45–67
doi:10.1006/jsvi.1999.2600, available online at http://www.idealibrary.com on IDEAL®

THEORETICAL CHARACTERISTICS OF THE VIBRATION OF SANDWICH PLATES WITH IN-PLANE NEGATIVE POISSON'S RATIO VALUES

F. SCARPA AND G. TOMLINSON

*Dynamics Research Group, Department of Mechanical Engineering, University of Sheffield, Sheffield S*1 3*JD, England*

(*Received* 4 *January* 1999, *and in final form* 21 *June* 1999)

This paper is concerned with re-entrant cell honeycombs which show in-plane negative Poisson's ratio values, in which their anisotropic mechanical properties are described using the cellular material theory. Out-of-plane shear moduli are affected by the unit cell geometric parameters and, for some ranges of the latter, it is possible to obtain higher values of the shear moduli compared to those of a regular hexagonal honeycomb, in particular for cell geometries with a negative Poisson's ratio. A first order sandwich plate theory is applied in order to obtain the fundamental frequencies of sandwich laminates in cylindrical bending and for the simply supported case. Sensitivities of the frequencies per unit mass versus the geometric cell parameters are also calculated. The results suggest that the dynamic performance of a sandwich structure could be significantly improved with a proper design of the unit cell shape of the honeycomb. In particular, re-entrant cell cores offer improvements in bending stiffness capabilities for particular cell parameter ranges.

1. INTRODUCTION

When a sample of material is stretched it is naturally expected that a contraction in the direction perpendicular to the stretching one will occur. The expectation arises from the fact that all naturally occurring materials appear to exhibit this property. The Poisson ratio is the quantity defining this fundamental material feature.

For an isotropic material the Poisson ratio is defined by

$$\nu = \frac{-\varepsilon_y}{\varepsilon_x}, \tag{1}$$

where ε_x is the tensile strain in the stretching direction and ε_y the tensile strain perpendicular to this. Since most materials contract in the perpendicular direction to the applied load the presence of a minus sign in the definition ensures a positive value of the ratio. On the contrary, a material with a negative Poisson's ratio expands in all directions when pulled in only one, leading to an increase of its volume. Evans [1] was the first to define such materials as auxetic, from the Greek

0022-460X/00/060045 + 23 $35.00/0

$\alpha\upsilon\xi\varepsilon\tau o\sigma$ (that may be increased), to avoid the cumbersome phrase "materials with negative Poissons ratio".

It has to be pointed out that the positive strain energy theory of isotropic elasticity allows the Poisson ratios in the range between -1 and 0·5. The upper limit of the Poisson ratio corresponds to a material that conserves its volume when stretched. For any value less than 0·5 the material undergoes some increase in volume during the deformation. From this point of view, negative Poisson's ratio values imply an unusual large increase of volume only, not involving any difference in deformation behaviour [2].

In recent years, auxetic isotropic polymers and foams were developed by cell-shape change from a convex polyhedron to a concave one. In addition to their negative Poisson's ratio properties, these new materials indicated enhancement in several properties such as impact absorption, damage resistance and tolerance, shear modulus and indentation resistance, compared to conventional foam materials and polymers with positive Poisson's ratio [4].

Honeycomb structures with inverted cells have been reported to have negative Poisson's ratio in the cell plane [2]. The linear elastic response of these honeycomb structures, both conventional and re-entrant, has been analyzed by Warren and Kraynik using a homogenization technique [3]. Gibson and Ashby [2] applied a beam theory to the unit cell in order to describe the linear elastic behaviour of conventional and general honeycombs. Evans [5] assessed experimentally the possibility of using the cellular material theory (CMT) of Gibson and Ashby to describe the linear elastic response of auxetic honeycombs, using a photographic technique to detect anticlastic bending deformations of re-entrant paper honeycomb samples. The same author showed as well that re-entrant cell honeycombs allow the manufacturing of double-curved sandwich panels without cell buckling [6].

In this paper the CMT is used to analyze the mechanical properties of auxetic honeycombs. From the theoretical framework it can be demonstrated that general honeycombs have orthotropic mechanical properties. This feature allows the use of first order sandwich plate theories [7] to describe the dynamic performance of sandwich structures with an orthotropic core. Fundamental natural frequencies of sandwich plates simply supported and in cylindrical bending are computed, as well as their sensitivities to geometry cell parameters. The importance of the geometric layout of the unit cell is stressed by the fact that the aspect ratios of the unit cells, as well as their internal cell angles and thickness of the cell walls define the magnitudes of Young's and shear moduli of the honeycombs and, moreover, the negative Poisson's ratio behaviour in the cell plane. As will be shown, it is the negative internal cell angle (i.e., a re-entrant unit cell layout) which causes the auxetic behaviour of the honeycomb. Negative Poisson's ratio values are thus a geometric effect, due to the reshape of the microstructure of the cellular material [5].

2. MECHANICAL PROPERTIES OF AUXETIC HONEYCOMBS

According to the CMT [1], the in-plane linear elastic response of general honeycombs can be described by the geometry of the unit cell and by considering

the walls of the cells as Euler–Bernoulli beams. The mechanical properties of a general honeycomb unit cell (Figure 1) can be described by the virgin core material properties and by three non-dimensional parameters: the internal cell angle θ, the aspect ratio of the cell sides $\alpha = h/l$, and the relative thickness $\beta = t/l$.

When the honeycomb is loaded in the directions X_1 or X_2 the cell walls bend [2]. The response in the cell plane is described by four independent moduli, due to the fact that the orthotropic relation in equation (2) holds [1]:

$$E_1 v_{21} = E_2 v_{12}. \tag{2}$$

Taking into account axial and shear deformation effects [2], the in-plane Poisson's ratio v_{12} can be computed as

$$v_{12} = \frac{\cos^2\theta}{(\alpha + \sin\theta)\sin\theta} \frac{1 + (1{\cdot}4 + 1{\cdot}5v_c)\beta^2}{[1 + (2{\cdot}4 + 1{\cdot}5v_c + \cot^2\theta)\beta^2]}, \tag{3}$$

where v_c is the Poisson ratio of the virgin core material. A detailed derivation of formula (3) is presented in Appendix A. A negative internal cell angle implies a re-entrant unit cell layout, like the one shown in Figure 2. From equation (3) it can be seen that the negative Poisson's ratio effect is due to the presence of the sine term in the denominator, thus for negative internal cell angles the values are negative as shown in Figure 3.

The Poisson ratio of the honeycomb is undetermined for $\alpha = -\sin\theta$. In reality, this condition is never achieved, because for geometric considerations the internal vertices of the cell are not allowed to touch during the deformation. Mathematically, this condition is described as

$$\theta_{min} = -\sin^{-1}\left(\frac{\alpha}{2}\right). \tag{4}$$

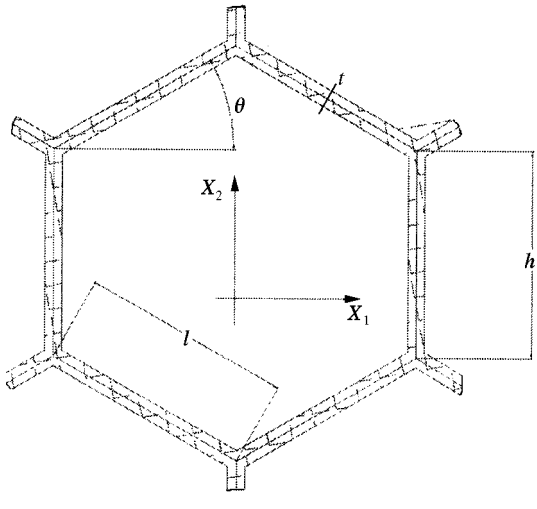

Figure 1. Unit cell layout for a regular honeycomb.

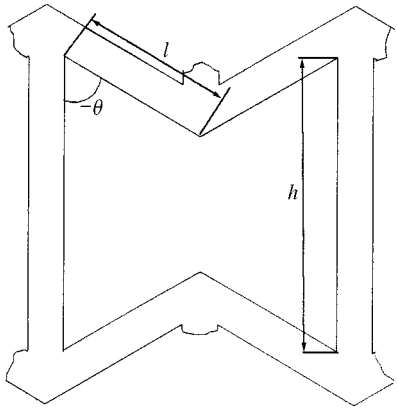

Figure 2. Unit cell layout of a re-entrant honeycomb.

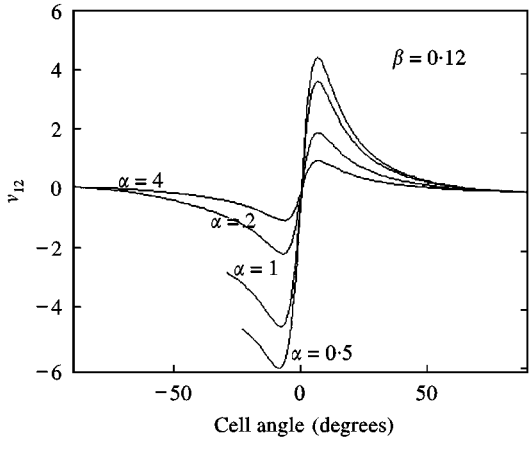

Figure 3. The Poisson ratio ν_{12} for various α values.

The in-plane Poisson's ratio ν_{12} is not symmetric for negative internal cell angles. It can be demonstrated that for a null internal cell angle (i.e., a condition approaching the rectangular cell honeycomb) the following is valid:

$$\lim_{\theta \to 0} \nu_{12} = 0. \tag{5}$$

Important design parameters for sandwich constructions are the out-of-plane shear moduli, which are responsible for the shear core resistance in bending behaviour for first order sandwich theory [7]. Two out-of-plane shear moduli are present for general anisotropic honeycombs. They can be calculated using the theorems of minimum potential energy and minimum complementary energy [2]. This approach results in a unique expression for the shear modulus G_{13}, where X_3 is the

normal direction to the plane X_1X_2; for G_{23} upper and lower bounds can be formulated [8]. Grediac [11] showed the dependency of the shear modulus G_{23} on the ratio between the thickness of the whole honeycomb and the length of the unit cell. His finite element analysis allows one to obtain a unique expression for G_{23}, intermediate between the upper and lower bounds calculated by energy approaches.

The out-of-plane shear moduli show interesting behaviour in the negative cell angle range. The ratio G_{13}/G_c, where G_c is the virgin core material shear modulus, increases significantly for increasing negative angles and low cell aspect ratios; while for higher values of α there is an opposite behaviour as shown in Figure 4. The ratio G_{23}/G_c shows a more symmetric behaviour for positive and negative cell angles, with decreasing values for low cell aspect ratios (Figure 5). It must be pointed out that for a regular honeycomb ($\alpha = 1$, $\theta = 30^\circ$) the upper and lower bounds for G_{23}/G_c coincide, leading with the following [2]:

$$(G_{23}/G_c)_{reg} = 0{\cdot}577\beta. \tag{6}$$

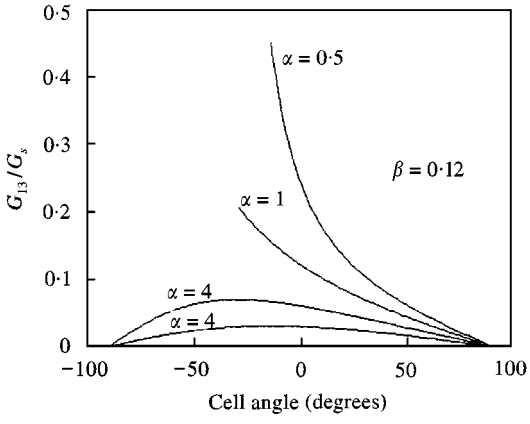

Figure 4. Out-of-plane shear modulus ratio G_{13}/G_s.

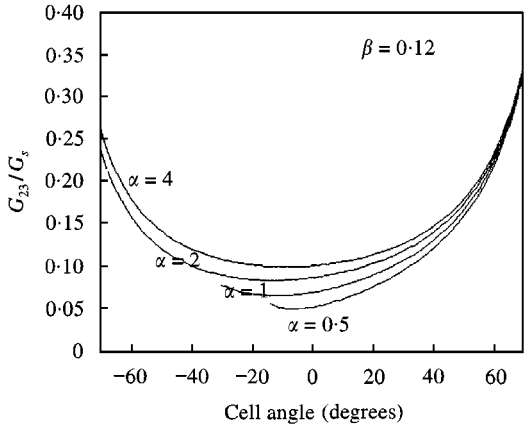

Figure 5. Out-of-plane shear modulus ratio G_{23}/G_s.

Equation (6) is well supported by experimental results obtained on aluminium and steel honeycombs [8].

The density ρ_H of a general honeycomb is also affected by the unit cell geometric parameters and the density of the virgin core. For low relative densities ($\beta < 0{\cdot}25$) the CMT states the following:

$$\frac{\rho_H}{\rho_c} = \frac{\beta(\alpha + 2)}{2\cos\theta(\alpha + \sin\theta)}, \tag{7}$$

where ρ_c is the density of the core material.

Figure 6 shows that for internal negative cell angles there is an increase of the density, compared to that of a regular honeycomb. This statement is valid in particular for low internal cell angles values and cell aspect ratios.

The honeycomb density scales linearly with the thickness of the wall cells (i.e., β), as well as the out-of-plane shear moduli. The other in-plane properties scale as β^2, and show high stiffness ratios in the directions X_1, X_2. Only for regular hexagonal cell honeycombs is the degree of anisotropy null [2].

3. ANALYSIS OF SANDWICH PLATES

3.1. CYLINDRICAL BENDING

For very high length-to-width ratios the sandwich plate deformations may be considered to be independent of the length co-ordinate. In cylindrical bending the laminate is of infinite length in one direction (y in this case), and uniformly supported along the opposite edges $x = 0, a$ (see Figure 7). The assumption of equal upper and lower face sheet thickness has been made in order to model a symmetric sandwich plate. Further simplification is imposed considering both the face sheets and core material as the same.

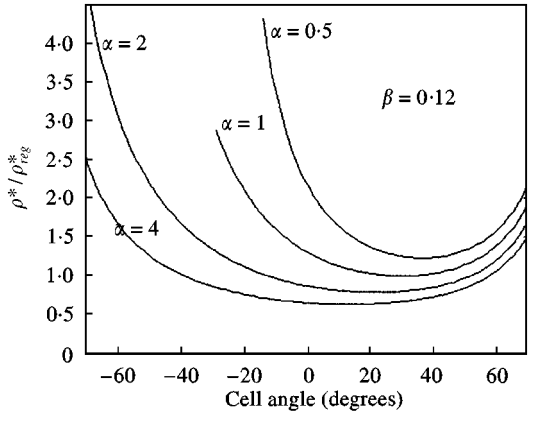

Figure 6. General honeycomb density versus internal cell angle.

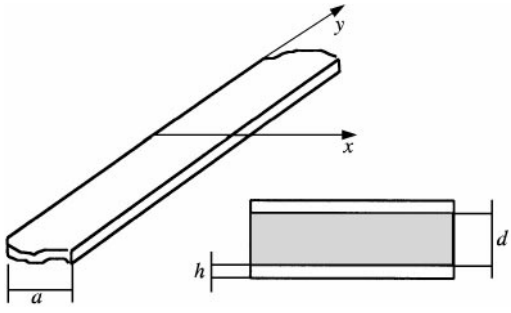

Figure 7. Sandwich plate in cylindrical bending.

From the formulation of Whitney [6, p. 302], assuming rotary inertia absence and null in-plane and normal loads, the following equations of motion hold:

$$D\frac{\partial^2\psi_x}{\partial x^2} - G_{13}d\left(\psi_x + \frac{\partial w}{\partial x}\right) = 0,$$

$$G_{13}d\left(\frac{\partial\psi_x}{\partial x} + \frac{\partial^2 w}{\partial x^2}\right) = \rho_t\frac{\partial^2 w}{\partial t^2}. \tag{8}$$

where d is the core thickness and ψ_x and w are, respectively, the rotation along the x-axis and the normal displacement. D is the bending stiffness of the laminate defined as

$$D = Es^3\frac{\gamma(\gamma+1)}{4(1-\nu^2)}, \tag{9}$$

where $\gamma = d/s$ and s is the face sheet thickness. The total mass ρ_t per unit area of the sandwich plate is

$$\rho_t = s(2\rho_c + \gamma\rho_H). \tag{10}$$

The static mechanical performance of auxetic sandwich laminates incylindrical bending is significantly improved using unit-cell cores with negative internal cell angles and specific aspect ratios [9]. Figure 8 shows the maximum central displacement per unit mass of a simply supported sandwich plate subjected to a uniform distributed pressure. Both the face sheet and core material is aluminium. For low negative cell angles and aspect ratios ($\alpha < 2$) the maximum central displacement is significantly reduced compared to the one of a sandwich plate with a regular core. This fact allows a consistent increase of the bending stiffness of the sandwich laminate.

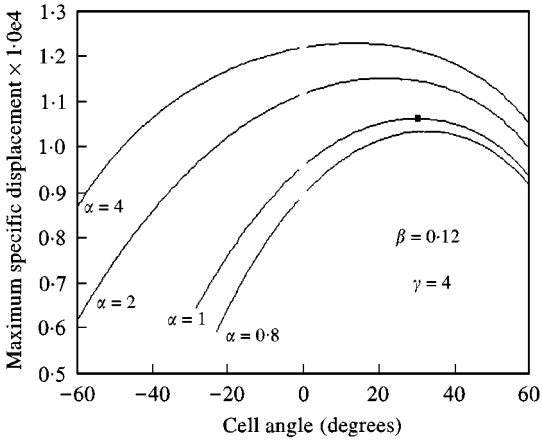

Figure 8. Non-dimensional maximum displacements for a sandwich plate in cylindrical bending. ■ Regular honeycomb.

For simply supported boundary conditions the generalized co-ordinates assume the following form [7, p. 308]:

$$w = A_m e^{i\omega_m t} \sin \frac{m\pi x}{a},$$

$$\psi_x = B_m e^{i\omega_m t} \cos \frac{m\pi x}{a}. \tag{11}$$

Substituting equation (11) into equation (8), one obtains an eigenvalue problem. The solution of the characteristic equation is

$$\omega_m = \bar{\omega}_m \sqrt{1 - \frac{Sm^2\pi^2}{1 + Sm^2\pi^2}}, \tag{12}$$

where

$$S = \frac{1}{2}\left(\frac{s}{a}\right)^2 \frac{(\alpha + \sin\theta)(\gamma + 1)}{\cos\theta(1 - \nu)\beta} \tag{13}$$

and

$$\bar{\omega}_m = \left(\frac{m\pi}{a}\right)^2 \sqrt{Es^3 \frac{\gamma(\gamma + 1)}{4\rho_t(1 - \nu^2)}}. \tag{14}$$

Expression (12) can be arranged in the following form:

$$\omega_m = \tilde{\omega}_m F_{geom} \tag{15}$$

where

$$\tilde{\omega}_m = \left(\frac{m\pi}{a}\right)^2 \sqrt{Es^2 \frac{\gamma(\gamma+1)}{\rho_c(1+\nu)}}, \tag{16}$$

$$F_{geom} = a\sqrt{\frac{\beta(\alpha+\sin\theta)\cos^2\theta}{[4\cos\theta(\alpha+\sin\theta)+\gamma(\alpha+2)\beta][2\beta a^2\cos\theta(1-\nu)+s^2m^2\pi^2(\gamma+1)(\alpha+\sin\theta)]}}. \tag{17}$$

F_{geom} is a non-dimensional quantity including the terms related to the geometry of the honeycomb and the sandwich plate. The value of equation (17) for a sandwich plate with regular honeycomb ($\alpha = 1$, $\theta = 30^\circ$) is

$$F^{reg}_{geom} = a\sqrt{\frac{1{\cdot}125\beta}{[5{\cdot}196+3\gamma\beta][1{\cdot}732a^2(1-\nu)+14{\cdot}8s^2m^2(\gamma+1)]}}, \tag{18}$$

where the suffix *reg* stands for a reference sandwich plate having a regular core. It is worth noting that, for a given sandwich core-thickness value, the ratio ω_1/ω_1^{reg} is equivalent to the quantity F_{geom}/F^{reg}_{geom}. The simulations for the cylindrical bending case were carried out for a plate having $a = 0{\cdot}5$ m, $s = 0{\cdot}001$ m and $\gamma = 12$. The honeycomb had a relative density $\beta = 0{\cdot}12$. Figure 9 shows the behaviour of F_{geom}/F^{reg}_{geom} for various internal cell angles and cell aspect ratios. For values of α lower than two, the geometric relation (4) holds. The curves in Figures 8 and 9 are limited by the value θ_{min} calculated from equation (4).

The ratio F_{geom}/F^{reg}_{geom} of the laminate is reduced for low θ values, as well as for low aspect ratios. With increasing values of α, the non-dimensional quantity assumes higher values compared to the ones of the reference laminate for very low internal

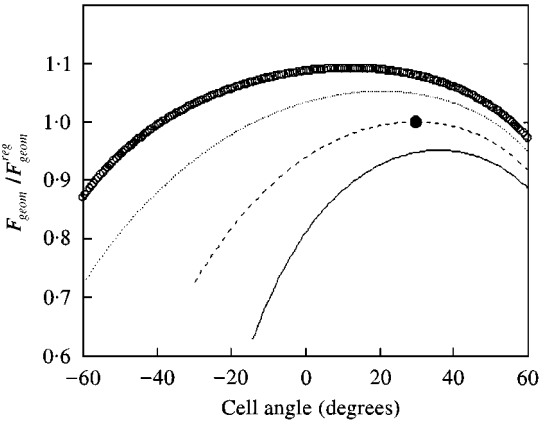

Figure 9. F_{geom}/F^{reg}_{geom} for various α values. ● Hexagonal honeycomb. ○ $\alpha = 4{\cdot}0$; ····· $\alpha = 2{\cdot}0$; - - - - $\alpha = 1{\cdot}0$; —— $\alpha = 0{\cdot}5$.

cell angles. This is due to the fact that in the same parameter range the density of an auxetic core is lower than that of a regular hexagonal honeycomb (Figure 6). For high negative cell angles, the increase of the density core is significant, while the shear modulus G_{13} is inferior to that of a regular honeycomb, thus leading to a decrease of the fundamental frequency of the laminate. It is worth noting that the honeycomb density is inversely proportional to the term $\alpha + \sin\theta$, which is present in the square root of the numerator of equation (17).

From Figure 9 the importance of the internal cell angle of the cell can be seen, as well as the cell aspect ratio α, on the dynamic properties of a sandwich laminate. From the design point of view it is interesting to investigate the sensitivity of the non-dimensional quantity (17) versus the geometric cell parameter of the unit cell. This can be achieved by calculating the following derivatives:

$$\frac{\partial F_{geom}}{\partial \theta}, \qquad \frac{\partial F_{geom}}{\partial \alpha}. \tag{19}$$

The quantities in equation (19) were obtained by means of the *MAPLE*© code [10].

Figure 10 shows the derivative of the parameter F_{geom} of the laminate versus the internal cell angle, for various aspect ratio values. The derivative is also plotted against the corresponding in-plane Poisson's ratio v_{12} (Figure 11). Depending on the α value, the sensitivity versus the cell angle changes sign for positive θ values, where the in-plane Poisson's ratio is positive. Within these values, F_{geom} reaches a maximum as can be observed from Figure 9. The importance of the cell aspect ratio α is more remarkable especially for negative internal cell angles, as shown in Figure 12 ($1{\cdot}1 \leqslant \alpha \leqslant 4$). Steep variations in sensitivity values are observed for low values of α, close to the limit condition defined in equation (4). For higher values, the sensitivity (and the in-plane Poisson's ratio v_{12}) tends to decrease (Figure 13), suggesting the fact that the dynamic behaviour of high aspect ratio cell honeycombs

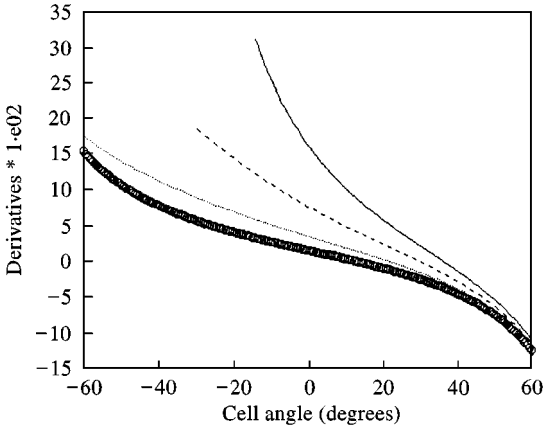

Figure 10. $\partial F_{geom}/\partial\theta$ for various α values. ○ $\alpha = 4{\cdot}0$; ····· $\alpha = 2{\cdot}0$; - - - - $\alpha = 1{\cdot}0$; —— $\alpha = 0{\cdot}5$.

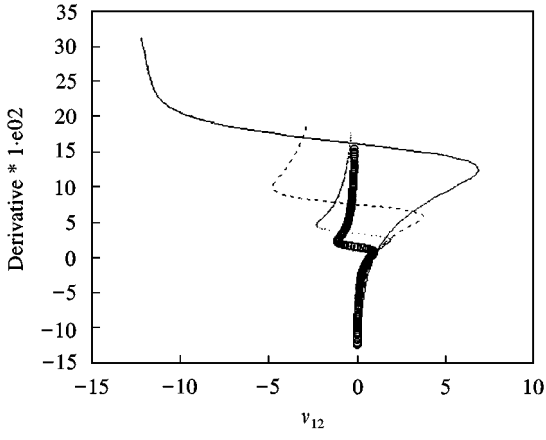

Figure 11. $\partial F_{geom}/\partial\theta$ versus v_{12}. ○ $\alpha = 4{\cdot}0$; ···· $\alpha = 2{\cdot}0$; - - - - $\alpha = 1{\cdot}0$; —— $\alpha = 0{\cdot}5$.

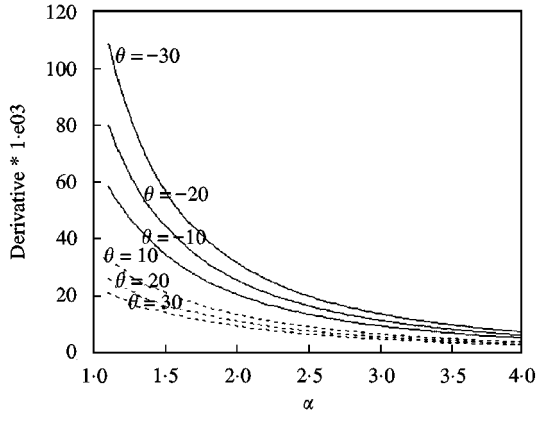

Figure 12. $\partial F_{geom}/\partial\alpha$ for various θ angles.

changes less significantly for a fixed internal cell angle value. This is particularly true for small internal cell angles, where the in-plane Poisson's ratio assume small values for high α ratios. The fact is explained by the weak dependence on the internal cell angle of the out-of-plane shear modulus G_{13} for high α values. At the same time, the density of the honeycomb is proportional to a factor $\beta(\alpha + 2)/2\alpha$, which tends to $\beta/2$ for very large aspect ratio values. Furthermore, the sensitivity of auxetic honeycombs versus the cell aspect ratio remains significantly higher compared to the one of positive cell angle honeycombs. From Figure 13 an increase up to 4 times can be noted for negative internal cell angles ($\theta = -30^\circ$).

3.2. SIMPLY SUPPORTED SANDWICH PLATE

The case of a simply supported sandwich plate with identical top and bottom face sheets with orthotropic properties can be described using the formulations of

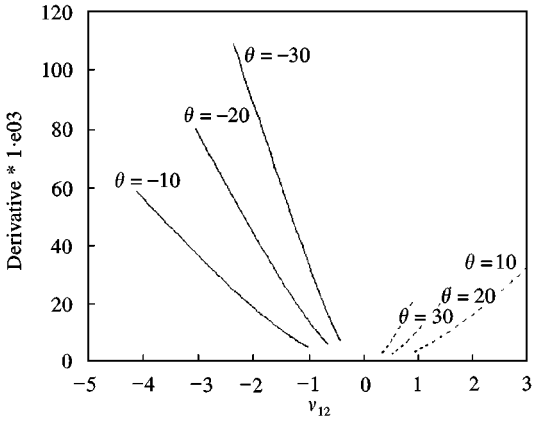

Figure 13. $\partial F_{geom}/\partial\alpha$ versus ν_{12}.

Whitney [7, p. 307] for a first order displacement theory. Neglecting the contributions of the in-plane loads, as well as the rotary inertia effects, the equations of motion are the following:

$$D_{11}\frac{\partial^2\psi_x}{\partial x^2} + D_{66}\frac{\partial^2\psi_x}{\partial y^2} + (D_{12} + D_{66})\frac{\partial^2\psi_y}{\partial x\partial y} - G_{13}d\left(\psi_x + \frac{\partial w}{\partial x}\right) = 0,$$

$$(D_{12} + D_{66})\frac{\partial^2\psi_x}{\partial x\partial y} + D_{66}\frac{\partial^2\psi_y}{\partial x^2} + D_{22}\frac{\partial^2\psi_y}{\partial y^2} - G_{23}d\left(\psi_y + \frac{\partial w}{\partial y}\right) = 0,$$

$$G_{13}d\left(\frac{\partial^2\psi_x}{\partial x^2} + \frac{\partial^2 w}{\partial x^2}\right) + G_{23}d\left(\frac{\partial^2\psi_y}{\partial y^2} + \frac{\partial^2 w}{\partial y^2}\right) = \rho_t\frac{\partial^2 w}{\partial t^2}. \tag{20}$$

In this case the reduced bending stiffness terms are

$$D_{11} = D_{22} = Es^3\frac{\gamma(\gamma+1)}{4(1-\nu^2)}, \qquad D_{12} = \nu D, \qquad D_{66} = Es^3\frac{\gamma(\gamma+1)}{8(1+\nu)}. \tag{21}$$

The following solutions satisfy the simply supported boundary conditions:

$$\psi_x = \bar{\psi}_x e^{i\omega t}\cos\frac{m\pi x}{a}\sin\frac{n\pi y}{b},$$

$$\psi_y = \bar{\psi}_y e^{i\omega t}\sin\frac{m\pi x}{a}\cos\frac{n\pi y}{b},$$

$$w = \bar{w}e^{i\omega t}\sin\frac{m\pi x}{a}\sin\frac{n\pi y}{b}. \tag{22}$$

Imposing equation (22) one obtains an algebraic eigenvalue system. For each combination of sine wave numbers in the xy plane, the natural frequency can be calculated imposing a zero value for the determinant of the equations.

From equation (14) it can be observed that the dynamic behaviour of the laminate is affected by the two out-of-plane shear moduli of the honeycomb core. Due to the degree of anisotropy G_{13}/G_{23}, the dimensions of the laminate are important to determine the mechanical performance of the whole laminate.

For the numerical simulations a square simply supported plate is considered, with a thickness ratio γ of 12, and face sheet thickness of 0·1 mm. The dimensions of the laminate are $a = b = 0{\cdot}5$ m. As in the case of cylindrical bending, both the face sheet and core material is aluminium ($E_c = 70$ GPa, $\nu = 0{\cdot}3$, $\rho_c = 2400$ kg/m^3).

A non-dimensional frequency was defined in the following way:

$$\omega_{11}^{ad} = \omega_{11} a^2 \sqrt{\frac{\rho_c \gamma s}{D_{11}}} = \omega_{11} a^2 \sqrt{\frac{4\rho_c(1-\nu^2)}{Es^2(\gamma+1)}}. \tag{23}$$

Figure 14 shows the non-dimensional frequency ω_{11}^{ad} versus the internal cell angle for various cell aspect ratios. The behaviour of the simply supported square laminate is similar to that of the sandwich plate in cylindrical bending. From Figure 15, for an aspect ratio of 0·5, the ratio G_{13}/G_{23} is about 4·0 around the null internal cell angle (where there is the highest level of anisotropy [2]). For the same aspect ratio, the maximum non-dimensional frequency is located around 35°, where the density ratio $(\rho_H/\rho_c)/\beta$ (from equation (7)), is about 1·42, at the lowest value. For higher α values, the maximum non-dimensional frequencies are located around the null internal cell angle, where both the ratio between the shear moduli and the core density reach their maximum and minimum values respectively.

The sensitivities of ω_{11}^{ad} are shown in Figures 16–19. For increasing positive internal cell angles (i.e., for positive in-plane Poisson's ratio values), the sensitivities

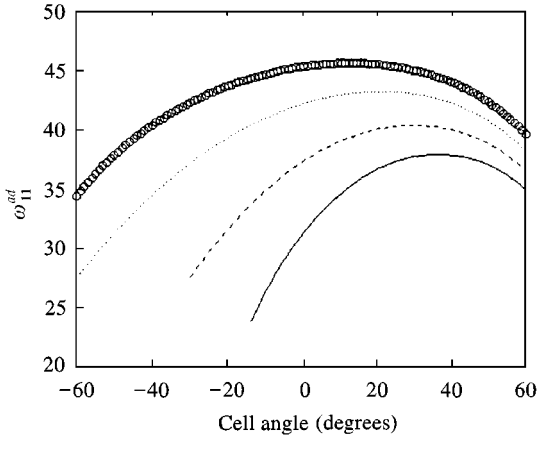

Figure 14. ω_{11}^{ad} versus cell angle. ○ $\alpha = 4{\cdot}0$; ···· $\alpha = 2{\cdot}0$; - - - - $\alpha = 1{\cdot}0$; —— $\alpha = 0{\cdot}5$.

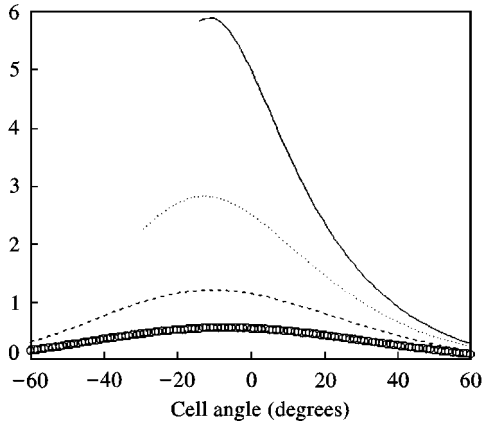

Figure 15. G_{13}/G_{23} versus cell angle. —— $\alpha = 0{\cdot}5$; ···· $\alpha = 1{\cdot}0$; - - - - $\alpha = 2{\cdot}0$; ○ $\alpha = 4{\cdot}0$.

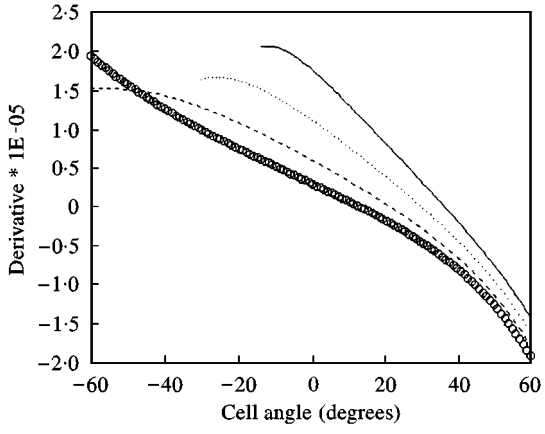

Figure 16. $\partial\omega_{11}^{ad}/\partial\theta$ for various cell aspect ratios. ○ $\alpha = 4{\cdot}0$; ···· $\alpha = 2{\cdot}0$; - - - - $\alpha = 1{\cdot}0$; —— $\alpha = 0{\cdot}5$.

of the fundamental non-dimensional frequency tend to the same values. For increasing cell aspect ratios, their is a shift of the peak sensitivity curve of ω_{11}^{ad} curves toward $\theta = 0^\circ$ (Figure 16). For negative cell angles, the sensitivities versus θ are always positive, with higher values for negative small cell angles and reduced α ratios (Figure 16). It is worth noting that in the same range of cell parameters the honeycomb has the higher magnitude values for the in-plane Poisson's ratio v_{12} (Figure 17). The sensitivity of ω_{11}^{ad} versus the cell aspect ratio is shown in Figure 18. For high α values, the curves for different cell angles show an asymptotic trend. Higher sensitivities are present for low cell aspect ratio values. Within this range ($1{\cdot}1 \leqslant \alpha \leqslant 2$), the difference between sensitivities increases for increasing cell angle magnitudes ($\theta = \pm 30^\circ$ in our case). This fact can be better observed in Figure 19.

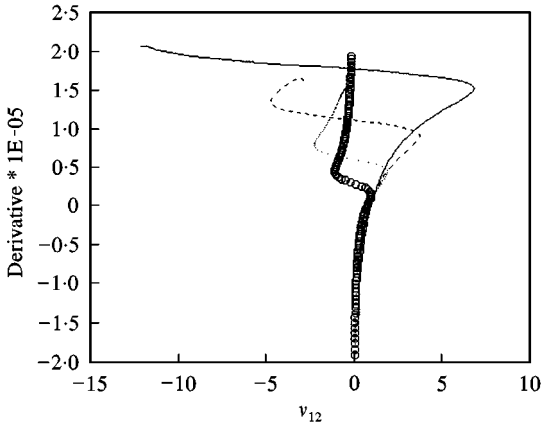

Figure 17. $\partial\omega_{11}^{ad}/\partial\theta$ versus ν_{12}. ○ $\alpha = 4{\cdot}0$; ···· $\alpha = 2{\cdot}0$; - - - - $\alpha = 1{\cdot}0$; —— $\alpha = 0{\cdot}5$.

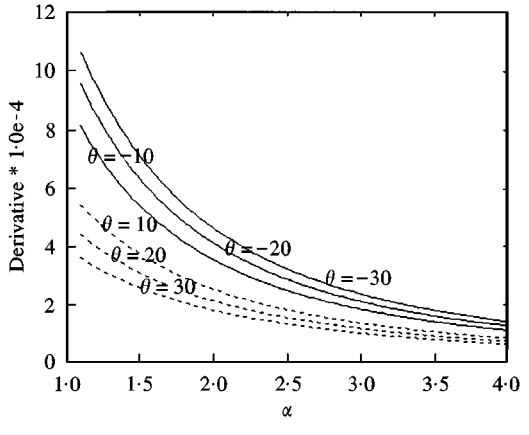

Figure 18. $\partial\omega_{11}^{ad}/\partial\alpha$ versus various cell angles.

The patterns of sensitivities for plates in cylindrical and general bending have some common similarities, although the non-dimensional quantities F_{geom} and ω_{11}^{ad} are intrinsically different. Furthermore, the similitude between the sensitivities can be noticed in Figures 12 and 18. For low internal cell angles ($-10^\circ \leqslant \theta \leqslant 10^\circ$) the difference between sensitivities for increasing α tends to decrease. In this parameter range the ratio of the out-of-plane shear moduli G_{13}/G_{23} ranges from 0·45 ($\alpha = 4{\cdot}0$, $\theta = -10^\circ$), to 5·8 ($\alpha = 0{\cdot}5$, $\theta = -10^\circ$), meaning that the stiffness behaviour is ruled mainly by the shear modulus G_{13}, as in the cylindrical bending case, for low cell aspect ratio values (Figure 15). Moreover, for α values close to zero, the honeycomb is composed of cells approaching the rectangular shape, where the degree of anisotropy is high and the bending behaviour of the cells is zero for certain directions of loading [2].

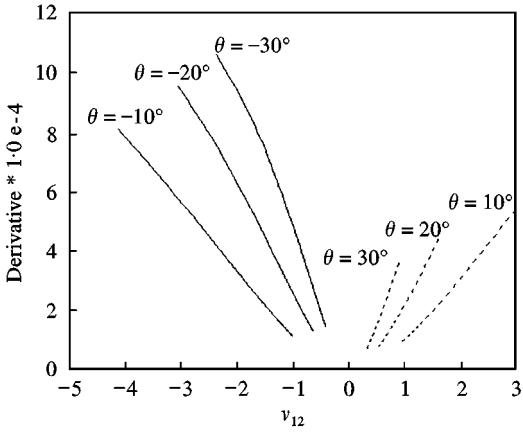

Figure 19. $\partial\omega_{11}^{ad}/\partial\alpha$ versus ν_{12}.

For higher aspect ratio values, the sensitivities have an asymptotic trend. This is explained by the significant aspect ratio dependence of the ratio G_{13}/G_{23} for high values of α, which leads to 0·24 on average for $45^\circ \leqslant \theta \leqslant 50^\circ$.

3.3. FREE VIBRATION OF GENERAL SANDWICH PLATE AND NUMERICAL COMPARISON

In the simplified models shown above, the in-plane and rotary inertia terms were neglected. The equations of motion for a general symmetric sandwich plate can be derived from the ones of a laminated plate undergoing shear deformation [7, p. 266]. Considering the vanishing of the bending-extensional coupling terms and in-plane loads, the equations of motion assume the following form:

$$A_{11}\frac{\partial^2 u}{\partial x^2} + A_{66}\frac{\partial^2 u}{\partial y^2} + (A_{12} + A_{66})\frac{\partial^2 v}{\partial x \partial y} = \rho_t \frac{\partial^2 u}{\partial t^2}$$

$$(A_{12} + A_{66})\frac{\partial^2 u}{\partial x \partial y} + A_{66}\frac{\partial^2 v}{\partial x^2} + A_{22}\frac{\partial^2 v}{\partial y^2} = \rho_t \frac{\partial^2 v}{\partial t^2},$$

$$D_{11}\frac{\partial^2 \psi_x}{\partial x^2} + D_{66}\frac{\partial^2 \psi_x}{\partial y^2} + (D_{12} + D_{66})\frac{\partial^2 \psi_y}{\partial x \partial y} - G_{23} d\left(\psi_x + \frac{\partial w}{\partial x}\right) = I\frac{\partial^2 \psi_x}{\partial t^2},$$

$$D_{66}\frac{\partial^2 \psi_y}{\partial x^2} + D_{22}\frac{\partial^2 \psi_y}{\partial y^2} + (D_{12} + D_{66})\frac{\partial^2 \psi_x}{\partial x \partial y} - G_{13} d\left(\psi_x + \frac{\partial w}{\partial x}\right) = I\frac{\partial^2 \psi_y}{\partial t^2},$$

$$d\left[G_{23}\left(\frac{\partial \psi_x}{\partial x} + \frac{\partial^2 w}{\partial x^2}\right) + G_{13}\left(\frac{\partial \psi_{yx}}{\partial y} + \frac{\partial^2 w}{\partial y^2}\right)\right] = \rho_t \frac{\partial^2 w}{\partial t^2}, \tag{24}$$

where $(A_{ij}, D_{ij}) = \int_{-h/2(\nu+1)}^{h/2(\nu+1)} C_{ij}(1, z^2)\,\mathrm{d}z$, and C_{ij} are the terms of the stress–strain matrix of the materials composing the sandwich. I is the inertia rotary term for the laminate.

Considering a simply supported sandwich plate, the following solutions are imposed:

$$u = \bar{u}_{mn} e^{i\omega t} \sin\frac{m\pi x}{a} \cos\frac{n\pi y}{b},$$

$$v = \bar{v}_{mn} e^{i\omega t} \cos\frac{m\pi x}{a} \sin\frac{n\pi y}{b},$$

$$\psi_x = \bar{\psi}_x e^{i\omega t} \cos\frac{m\pi x}{a} \sin\frac{n\pi y}{b},$$

$$\psi_y = \bar{\psi}_y e^{i\omega t} \sin\frac{m\pi x}{a} \cos\frac{n\pi y}{b},$$

$$w = \bar{w} e^{i\omega t} \sin\frac{m\pi x}{a} \sin\frac{n\pi y}{b}. \tag{25}$$

Introducing equation (24) into equation (23), one obtains a set of homogeneous equations. In order to obtain non-trivial solutions, the determinant of the correspondent (5×5) system matrix is set to zero. For every combination of half-sine wavenumbers mn one obtains five natural frequencies.

A finite element model was prepared using the ANSYS© Rel. 5·4 code [12] to assess the validity of the results provided by the analytical approach. A square plate of length of 0·5 m, with total thickness 0·0042 m ($\gamma = 20$) was represented by a mesh of 144-layered elements SHELL91 with the sandwich option [12]. The material of the face sheet and the virgin core is aluminium (Young's modulus $E = 70$ GPa, density $\rho = 2400$ kg/m^3 and Poisson ratio $\nu = 0{\cdot}3$). The relative density of the core was $\beta = 0{\cdot}12$. The orthotropic material properties of the core were computed using the CMT formulas for general honeycombs [2]. A subspace iteration technique with a basis of eight vectors was adopted to compute the fundamental natural frequency of the laminate. The comparison between the analytical and numerical results is shown in Table 1.

4. SOUND TRANSMISSION THROUGH A CYLINDRICAL SANDWICH SHELL

The use of high strength-to-weight ratio materials in transport aircraft may result in increased interior noise levels. Koval [13] showed that more noise could be transmitted through laminated fibre-reinforced structures than through isotropic ones in the frequency range from 1 to 10 times the ring frequency of the shell. Sandwich structures with honeycomb cores are still widely used in aerospace

TABLE 1

Fundamental frequency ω_{11} of a simply supported sandwich plate with different core cell aspect ratios and internal cell angles

α	θ (deg)	FEM (Hz)	Analytical (Hz)
2	−10	49·200	49·427
2	−20	46·877	47·055
2	−30	44·221	44·350
3·5	−10	52·768	52·957
3·5	−20	51·300	51·523
3·5	−30	49·458	49·811
4	−10	53·418	53·628
4	−20	52·086	52·360
4	−30	50·374	50·808

applications. Their acoustic properties are generally poor, outweighing their high stiffness-to-weight capabilities. Auxetic honeycombs, due to their improved stiffness ratios, could offer some advantages in sound reduction applications. Koval showed that a general orthotropic shell, below the ring frequency, has improved sound reduction capabilities due to the fact that in that region the acoustic behaviour tends to be stiffness governed. Choosing the appropriate set of geometric cell parameters, a re-entrant cell honeycomb offers enhanced out-of-plane mechanical properties, thus suggesting a possible application for sound reduction in fuselages and duct liners.

To analyze the acoustic properties of an infinite sandwich orthotropic shell immersed in a fluid medium the approach of Tang [15] is followed. The orthotropic shell is described by the Greenberg–Stavsky-type theory, where shear deformation is taken into account [13]. The interior of the shell is totally absorptive, and the shell is subjected to an external airflow at two independent incident angles. The acoustic properties of the system are described by the transmission loss quantity [13]:

$$TL = -10\,\mathrm{Log}_{10}\frac{W^T}{W^I}, \tag{26}$$

where W^T is the transmitted power and W^I the incidence power per unit length of axial section of the shell. Using the approach of Tang an explicit expression of the frequency spectrum of equation (25) is derived in terms of the modal impedance of the fluid and the shell.

Figure 20 shows the case of a typical narrow-bodied jet fuselage made of a sandwich shell, with a regular honeycomb and auxetic ones ($\alpha = 0{\cdot}8, 1$, $\beta = 0{\cdot}12$, $\theta = -10^\circ$). The shell radius is $R = 1{\cdot}83$ m, and the total thickness of the shell is 0·00736 m. A core-face sheet thickness ratio γ of 9·5 is assumed. Both face sheet and virgin core materials are aluminium. The shell is pressurized at 3150 m

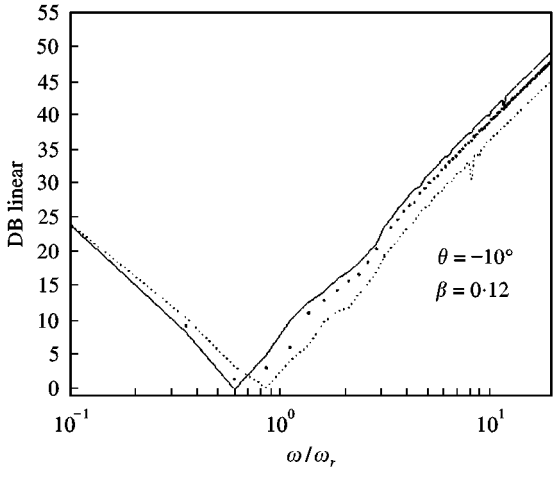

Figure 20. Transmission loss factors for sandwich shells with regular and auxetic cores. ···· Hexagonal; . . . . alpha = 1; —— alpha = 0·8.

(corresponding to 10 000 ft, with air density equal to 0·9041 kg/m^3 and speed of sound of 328·558 m/s). Exterior fluid with incident angles of 0 and 150° is at the same conditions of the one inside the shell. The exterior fluid is considered at rest (null Mach number). The frequency spectrum of the transmission loss factors is analyzed in the range from 0·1 to 20 times the ring frequency of a corresponding isotropic shell [15]. The ring frequency $\omega_r = (2\pi R)^{-1}\sqrt{E/\rho}$ is 445 Hz.

As seen in Figure 20, over the ring frequency the transimission loss factors of a sandwich shell with an auxetic core are higher than the ones of a sandwich shell with regular honeycomb. The fact is explained recalling that for low cell aspect ratios and negative internal cell angles the out-of-plane shear modulus G_{13} is higher than that of a hexagonal regular honeycomb (2·06 times) [9]. The bending stiffness of the laminate is thus increased, allowing a better acoustic performance in the frequency range where the behaviour is stiffness ruled. Although an auxetic sandwich shell shows improved bending stiffness capabilities, the increase of the core density results in an acoustic behaviour in the low range of frequencies (below the ring one), which is similar to that of a regular honeycomb sandwich structure.

6. CONCLUSIONS

Negative Poisson's ratio honeycombs constitute a novel class of material for sandwich structures. Choosing the appropriate geometrical cell layout, it is possible to obtain increased values of out-of-plane mechanical properties compared to the ones of a regular honeycomb. This fact leads to the possibility of having increased bending stiffness capabilities, an attractive feature for lightweight structures. For some particular combinations of cell angle and aspect ratio, enhanced strength

properties are followed by an increase of the density of the honeycomb, thus leading to a decrease of the natural frequencies of the structural system. The stiffness-ruled features of sandwich structures with auxetic core could be advantageously employed in structural components where low cut-off frequency behaviour is required. The increase of bending stiffness of a sandwich laminate with an auxetic core would allow the design of a statically stiff yet dynamically more complaint structure. As an example, sandwich components where sound transmission properties are demanding, especially for medium and high ranges of frequencies, could benefit from the use of a negative Poisson's ratio core.

ACKNOWLEDGMENTS

This work was supported by the Engineering and Physical Sciences Research Council under the ROPA Grant RA66033. The authors thank the anonymous referees for their helpful suggestions

REFERENCES

1. K. E. Evans 1995 *Journal of Material Science* **30**, 3319–3332. Microstructural modelling of auxetic microporous polymers.
2. L. J. Gibson and M. F. Ashby 1997 *Cellular Solids*: *Structure & Properties*. Oxford: Pergamon Press.
3. W. E. Warren and A. M. Kraynik 1987 *Mechanics of Materials* **6**, 27–31. Foam mechanics: the linear elastic response of two-dimensional spatially periodic cellular materials.
4. K. E. Evans and K. L. Alderson 1992 *Journal of Material Science Letters* **11**, 1721–1724. The static and dynamic moduli of auxetic microporous polyethylene.
5. B. D. Caddock, K. E. Evans and I. G. Masters 1991 *Proceedings of the ICCM*/8, *Honolulu*, *Section* 1-11, 3-E. Honeycomb cores with a negative Poisson's ratio for use in composite sandwich panels.
6. K. E. Evans 1991 *Computers & Structures* **17**, 95–111. Design of doubly curved sandwich panels with honeycomb cores.
7. J. M. Whitney 1987 *Structural Analysis of Laminated Anisotropic Plates*. Lancaster, PA: Technomic Publishing Company Inc.
8. S. Kelsey, R. A. Gellatly and B. W. Clark 1958 *Aircraft Engineering* **30**, 294–302. The shear modulus of foil honeycomb core.
9. F. Scarpa and G. Tomlinson 1998 *Proceedings of the Fourth European and Second MIMR*, *Harrogate*, *U.K.*, 559–566. On static and dynamic design criteria of sandwich plate structures with a negative Poisson's ratio core.
10. B. Char, K. O. Geddes et al. 1991 *Maple V Language Reference Manual*. New York: Springer-Verlag.
11. M. Grediac 1993 *International Journal of Solids and Structures* **30**, 1777–1788. A finite element study of the transverse shear in honeycomb cores.
12. *ANSYS Rel.* 5.4 *Element Manual* 1998 SAS IP Inc.
13. L. R. Koval 1979 *Journal of Sound and Vibration* **71**, 523–530. Sound transmission into a laminated composite cylindrical shell.
14. J. B. Greenberg and Y. Stavsky 1980 *Acta Mechanica* **37**, 13–28. Vibration of axially compressed laminated orthotropic cylindrical shells, including transverse shear deformation.

15. Y. Y. TANG, R. J. SILCOX and J. H. ROBINSON 1996 *Proceedings of the* 14*th International Modal Analysis, Dearborn, MI*, 1488–1495. Sound transmission through a cylindrical shell with honeycomb core.

APPENDIX A

Following reference [2], after a loading in the X_1 direction, the cell wall bends. The cell on itself is treated as a beam of length l, thickness t, depth b and Young's modulus E_c. The moment M tending to bend the cell wall is

$$M = \frac{Pl \sin \theta}{2}, \tag{A.1}$$

where (see Figure 21)

$$P = \sigma_1 (h + l \sin \theta) b. \tag{A.2}$$

From standard beam theory

$$\delta = \frac{Pl^3 \sin \theta}{12 E_c I}. \tag{A.3}$$

The shear deflection of the member is

$$\delta_s = \frac{Pl^3 \sin \theta}{12 E_c I} (2{\cdot}4 + 1{\cdot}5 v_c) \left(\frac{t}{l}\right)^2. \tag{A.4}$$

An axial load of $P \cos \theta$ acts on the member and the axial deflection is

$$\delta_a = \frac{Pl \cos \theta}{E_c t b}. \tag{A.5}$$

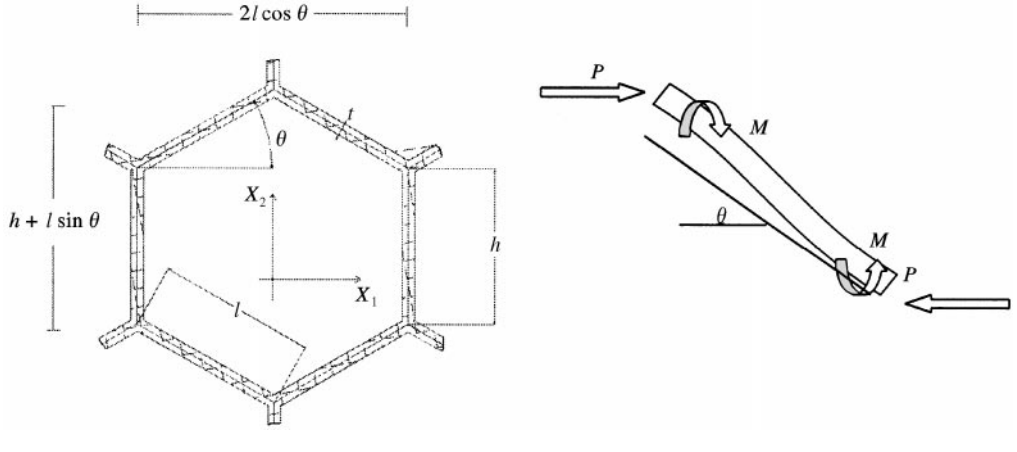

Figure 21. Unit cell layout and wall loading in the X_1 direction.

The total deflection in the X_1 direction is then

$$\delta_1 = \delta \sin\theta + \delta_s \sin\theta + \delta_a \cos\theta = \frac{Pl^3 \sin^2\theta}{12E_cI}\left(1 + (2{\cdot}4 + 1{\cdot}5\nu_c + \cot^2\theta)\left(\frac{t}{l}\right)^2\right). \quad (A.6)$$

The relative strain is

$$\varepsilon_{11} = \frac{\delta_1}{l\cos\theta}. \quad (A.7)$$

The elastic deformation in the X_2 gives similarly the following deflection:

$$\delta_2 = \delta \cos\theta + \delta_s \cos\theta - \delta_a \sin\theta = \frac{Pl^3 \sin\theta\cos\theta}{12E_cI}\left(1 + (2{\cdot}4 + 1{\cdot}5\nu_c - 1)\left(\frac{t}{l}\right)^2\right) \quad (A.8)$$

with the relative strain,

$$\varepsilon_{22} = -\frac{\delta_2}{h + l\sin\theta}. \quad (A.9)$$

Recalling the meaning of α and β, and applying the definition of the Poisson ratio value we obtain

$$\nu_{12} = -\frac{\varepsilon_{22}}{\varepsilon_{11}} = \frac{\cos^2\theta}{(\alpha + \sin\theta)\sin\theta}\frac{1 + (1{\cdot}4 + 1{\cdot}5\nu_c)\beta^2}{1 + (2{\cdot}4 + 1{\cdot}5\nu_c + \cot^2\theta)\beta^2}. \quad (A.10)$$

APPENDIX B: NOMENCLATURE

θ	internal cell angle
α	cell aspect ratio
β	honeycomb's relative density
E_1	in-plane Young's modulus in the direction X_1
E_2	in-plane Young's modulus in the X_2 direction
ν_{12}	in-plane Poisson's ratio
G_{13}	transverse shear modulus in the plane X_1X_3
G_{23}	transverse shear modulus in the plane X_2X_3
ρ_c	density of the virgin core material
ν_c	Poisson ratio of the virgin core material
E_c	Young's modulus of the virgin core material
G_c	$E_c/2(1 + \nu_c)$
ρ_H	density of the general honeycomb
d	core thickness
s	sandwich face sheet thickness
γ	d/s

D	bending stiffness of the sandwich plate $= Es^3[\gamma(\gamma + 1)/4(1 - v_c^2)]$
A_{ij}	orthotropic plate coefficients, equation (24)
D_{ij}	orthotropic reduced bending plate coefficients, equations (20)–(24)
u, v, w, ψ_x, ψ_y	plate rotation and displacement components
ω_{mn}	natural frequency mn of the plate
a, b	dimensions of the sandwich plate
R	sandwich shell radius
ω_r	ring frequency $= (2\pi R)^{-1}\sqrt{E/\rho}$